Co-PRECIPITATION SYNTHESIS, CHARACTERIZATION OF $CoFe_2O_4$ NANOMATERIAL AND EVALUATION OF ITS TOXICITY BEHAVIOR ON HUMAN LEUKEMIA CANCER K562 CELL LINE

LEILA KAFI-AHMADI [1], SHAHIN KHADEMINIA [2], MEHRIN NAJAFZADEH NANSA [3], ABDOL ALI ALEMI [4], MAJID MAHDAVI [5] AND AHMAD POURSATTAR MARJANI [6]*

[1]*Department of Inorganic Chemistry, Faculty of Chemistry, Urmia University, Urmia, Iran*
[2]*Department of Inorganic Chemistry, Faculty of Chemistry, Semnan University, Semnan, Iran*
[3]*Department of Chemistry, Faculty of Science, Payame Noor University, Tabriz, Iran*
[4]*Synthesis and Investigation Lab of Nano Materials, Faculty of Chemistry, University of Tabriz, Iran*
[5]*Department of Biology, Faculty of Natural Science, University of Tabriz, Tabriz, Iran*
[6]*Department of Organic Chemistry, Faculty of Chemistry, Urmia University, Urmia, Iran*

ABSTRACT

In this study, cobalt ferrite nanomaterial with inverse spinel structure was synthesized via a co-precipitation method using $Co(NO_3)_3.6H_2O$ and $Fe(NO_3)_3.9H_2O$. A 15% NH_4OH solution was used as an alkaline agent for pH adjustment. Oleic acid was used as a coating agent on the surface of the synthesized cobalt ferrite nanoparticles. PXRD analysis confirmed that the obtained material had a main $CoFe_2O_4$ cubic crystal structure with space group Fd-3m and lattice parameters a=b=c= 8.40 Å (JCPDS standard card no = 01-077-0426). According to the SEM analysis, the pseudo-spherical particles size distribution and morphology of the as-synthesized nanomaterial were homogeneous. The magnetic behavior of the obtained material was analyzed by vibrating-sample magnetometer (VSM). Besides, anti-cancer effect of the as-synthesized cobalt ferrite nanoparticles was examined on an experimental model of acute myeloid leukemia (CML) K562 cell line for the first time. Inhibition of cell growth and cytotoxicity (apoptosis) that are characteristics features of cobalt ferrite nanoparticles are tested on K562 cell line. The results showed growth and viability inhibition and induction of apoptosis in K562 cells treated with the nanoparticles.

Keywords: Chronic Myeloid Leukemia (CML), CoFe2O4, Co-precipitation; K562 cell, Nanoparticles.

1. INTRODUCTION

Ferrite materials refer to those magnetic materials that consist of iron(III) oxide as their fundamental constituent. Considerable magnetic parameters such as magnetic permeability and high electrical resistivity (about 1012 Ωcm) are of the characteristic features of these materials. So, they have found a wide range of applications in the fields of electricity, electronics, telecommunications, computer, etc [1-5]. Cobalt is a hard ferromagnetic element. Cobalt is used in many applications in magnets and magnetic recording media, used as a catalyst in chemical and oil industry, and as a drying agent for paints and wives [6]. $CoFe_2O_4$ as a ferromagnetic material possesses high magneto-crystalline anisotropy (a positive anisotropy constant), high magnetic coercively, an average magnetism, mechanical rigidity, chemical stability, and electrical resistance. It is a suitable candidate for many applications same as high frequency magnetics, information storage systems, magnetic fluids, black magnetic cores, drug delivery systems, magnetic resonance imaging (MRI), and biosensors [7,8]. There are several methods for the preparation of the magnetic compound including: co-precipitation [9-17], combustion [18-20], hydrothermal [21], sol-gel [22-24], microwave [25], etc.

Modifying the surface of magnetic nanoparticles (MNP) has many advantages. Coating MNP surface increases their lifetime by postponing the clearance, affects the surface hydrophobicity, surface charge and pH of the particles. Besides, surface modification provides the possibility of attaching antibodies or small molecules that can lead to specific binding to the target tissue. The organic and inorganic coating on the surface of nanoparticle prevent opsonization of them by macrophages. Uncoated magnetic nanoparticles are quickly removed by mononuclear phagocyte cells [6]. 15 to 20% of all of the leukemia are of CML type that is seen in children [26]. CML is one of the most common blood cancers and is considered as a stem cell failure caused by massive increase in abnormal stem cells in bone marrow which finally results in an abnormal decrease in the number of white and red blood cells. This leukemia is associated with abnormalities of chromosome 22 known as Philadelphia chromosome which is responsible for the creation of BCR-ABL abnormal gene. This gene makes an abnormal protein called thyroxin Echinacea which is believed to be the reason for the growth of the leukemia cells [27]. Apoptosis or programmed cell death with features such as cell shrinkage, formation of apoptotic bodies and chromosomal DNA fragmentation are critical in embryonic development and maintenance of homeostasis [28]. Defect in the process of apoptosis is the cause of many diseases, including cancer [29]. In recent years great efforts have been applied to find new compounds, especially of natural products that exert their anti-cancer features through induction of apoptosis in cancer cells [30]. Since the induction of apoptosis is an appropriate way to remove the cancer cells and since most of the cancer cells suffer defects in their apoptotic mechanisms, finding compounds that induce apoptosis in cancer cells is a research priority [31]. MTT test can be used to determine the toxicity of a substance for cells. In the present study, a facile co-precipitation route is explored for the synthesis of $CoFe_2O_4$ nanomaterial using the reaction between $Co(NO_3)_3.6H_2O$ and $Fe(NO_3)_3.9H_2O$ at a controlled pH medium. PXRD analysis is applied for the characterization of the obtained target. The surface modification is performed by oleic acid. FT-IR analysis is used to confirm the deposition of the coat on the surface of the particles. The magnetic behavior of the obtained nanomaterial is studied by VSM analysis. K562 cell line is used as the experimental model of chronic myeloid leukemia (CML) in the present work to study the anti-cancer property of the obtained sample.

2. EXPERIMENTAL

2.1. Material and methods

$Co(NO_3)_3.6H_2O$ and $Fe(NO_3)_3.9H_2O$ (as powders), and oleic acid solution were purchased from Merck Company. RPMI-1640 cultivation medium and fetal bovine serum (FBS) were obtained from Bios era England. Streptomycin and penicillin antibiotics and MTT powder and dimethyl sulfide (DMSO) were purchased from the Coinage Company. Trepan blue and ethidium bromide (EtBr) and Acridine Orange (AO) were purchased from Sigma-Aldrich, Germany. Cell line K562 for cell culture was obtained from the Pasteur Institute of Iran. FT-IR spectra were obtained as KBr plates on a FT-IR Shimadzu spectrophotometer in the 400–4000 cm^{-1} range. PXRD pattern of the complex was recorded using Bruker AXS diffractometer D8 Advance with Cu-Kα radiation with nickel beta filter in the 2θ range of 20-70°. The SEM images were collected by a Philips XL-30 FE-SEM. The magnetization curve under the external magnetic field was measured by JafcoSP620-Japen.

2.2. Preparation of cobalt ferrite nanoparticles

In a typical synthesis experiment, 146 mg of $Co(NO_3)_3.6H_2O$ (Mw = 291.03 $gmol^{-1}$) and 404 mg $Fe(NO_3)_3.9H_2O$ (Mw = 404.00 $gmol^{-1}$) were dissolved in 50 mL deionized water in two beakers, separately. The solutions were poured into beaker and mixed by magnetic stirring for 1 min. Then, 4.5 mL of 25% v/v NH_4OH solution was added to the resultant solution to justify the pH at 9. The obtained solution was stirred more for 5 min. Then, the solution was relaxed at room temperature until a precipitate was formed. The obtained precipitate was filtered and dried at room temperature for 24 h. Afterwards, the obtained precipitate was transferred into a 25 mL crucible and treated thermally at 650 ºC

*Corresponding author email: l.kafiahmadi@urmia.ac.ir

for 4 h in a furnace. After the process was finished, the crucible was cooled normally to the room temperature (S_1). The characterization of the resulting cobalt ferrite, purity and the size of the particles (nano-sized particles) were performed by PXRD. The obtained cobalt ferrite was added into a 100 mL of 45% v/v (distilled water/oleic acid) solution. The mixture was stirred at room temperature for 1 h until the coating process was completed. By centrifuging the solution, two-phases were separated. The first one was larger particles that were deposited at the bottom of the flask, and the smaller particles were in the suspension form in the supernatant phase which were collected and analyzed using FT-IR spectroscopy to confirm the successful coating process of the particles with oleic acid (S_2).

2.3. Cells cultures

In order to accomplish the cultivation, the purchased cells were cultivated and preserved in a RPMI 1640 (Biosera, England) medium in cell culture incubator at 37 °C, 95% relative humidity, and 5% CO_2 concentration, and were enriched with a 10% fetal bovine serum (FBS) (Biosera, England) as a growth factor for cells, antibiotics, penicillin (100 U/mL) and streptomycin (100 mg/mL) (Coinage, Tehran) to prevent contamination of the culture medium. The K562 cells were passaged and the medium was replaced every 24 h.

2.4. Toxicity of cobalt ferrite nanoparticles on K562 cells

To evaluate the cytotoxic effects of cobalt ferrite nanoparticles on K562 cells, MTT assay test was used. For the purpose, the cells were seeded in 96-well plates and 2×10^4 cells were plated in each cell. After 24 h, different dosages of the compound were added to each cell for 24, 48 and 72 h. All data obtained from this study were tested independently for three times. The resulting data were analyzed by SPSS 16, and Microsoft Excel 2010, and Student t-test. The data with p value less than 0.05 were significant.

3. RESULTS AND DISCUSSION

3.1. Characterization

Fig. 1a, shows the PXRD pattern of the as-prepared cobalt ferrite nanomaterial. The presence of 111, 220, 311, 400, 422, 440 and 511 miler planes in the PXRD patterns are attributed to the inverse cubic spinel structure with the space group Fd-3m and lattice parameter a=b=c= 8.40 Å (JCPDS standard card no = 01-077-0426). Fig. 1b, shows the PXRD pattern of the obtained material after coating by oleic acid. According to the pattern, it is obvious that the peak width of the as-prepared sample is more than pure $CoFe_2O_4$ when it is modified by oleic acid. So, the modification makes the crystallite sizes smaller than the pure $CoFe_2O_4$ nanomaterial.

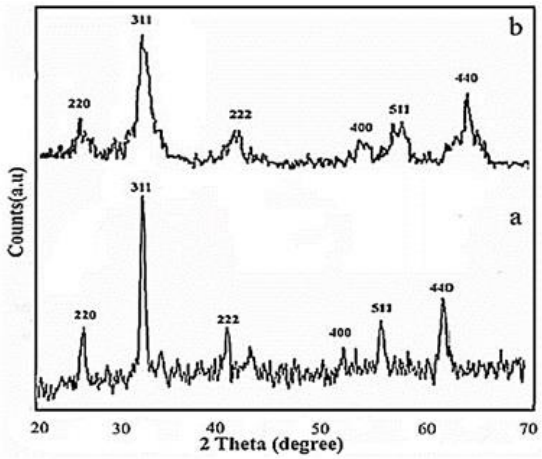

Figure 1. PXRD patterns of S_1 (**a**), and S_2 (**b**).

Fig. 2a and 2b, shows the FT-IR spectra of S_1, and S_2, respectively. According to the obtained spectra, two notable metal-oxygen bands, ν_1 and ν_2, can be observed. The band ν_1 is observed at a higher frequency and band ν_2 with lower frequency is attributed to the vibrations of M_{tetra}-O, and oxygen ion and M_{octa}-O bonds, respectively. The absorption bands at 355 and 579 cm^{-1} are corresponded to Co-O and Fe-O vibration bands that the appearance of such peaks confirms the formation of the spinel structure [10,18]. Fig. 2a, shows two strong absorption bands at 434 and 592 cm^{-1} assigned to stretching vibrations of Co-OR and Fe-O bands present in octahedral and tetrahedral cavities, respectively. Fig. 2b, shows that there are some absorption bands at 584, 676, 719, 941, 1456 and 1708 cm^{-1}. The peaks at 584 and 676 cm^{-1} are attributed to stretching vibrations of Co-O and Fe-O bands present in octahedral and tetrahedral cavities, respectively. The absorption band at 1456 cm^{-1} is assigned to the bending vibrations of OH groups of physically adsorbed water. Additionally, the absorption band at 1708 cm^{-1} corresponded to the carbonyl group of oleic acid [32-34].

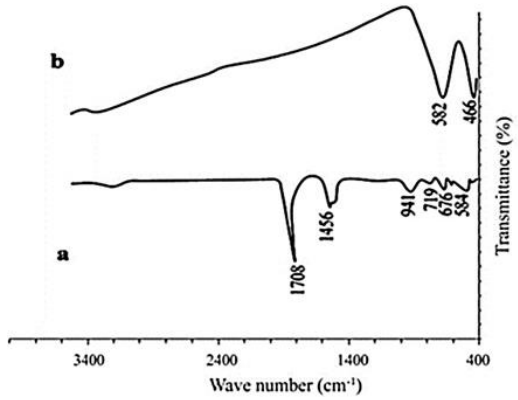

Figure 2. FT-IR spectra of S_1 (**a**), and S_2 (**b**).

Fig. 3a and 3b, presents the SEM image as well as particle size distribution profile of S_2, respectively. The data show that the material is composed of nanoparticles. The particle size distribution profile is shown in Fig. 3b, reveals that the maximum particle size distribution is in the range of 25–30 nm.

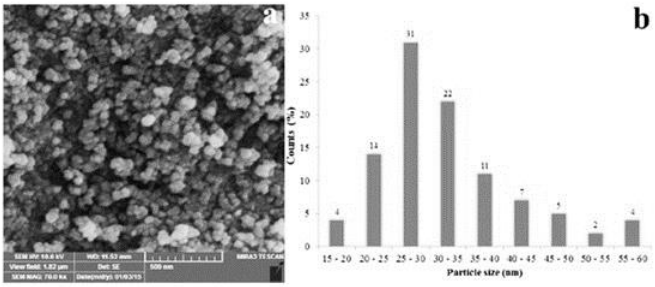

Figure 3. SEM image (**a**), and particle size distribution profile of S_2 (**b**).

The chemical composition of sample surface shown in Fig. 4 was analyzed by energy dispersive X-ray spectroscopy (EDX). The obtained spectrum of the as-prepared coated nanomaterial is presented as a function of Fe, Co, C, N and O elements concentrations. It can be found that the X-rays emitted from different elements indicate the existence of Fe, Co, C, N and O atoms. Besides, the related energy positions and the specific X-ray lines obtained from elements confirm the successful synthesis of $CoFe_2O_4$ nanomaterials.

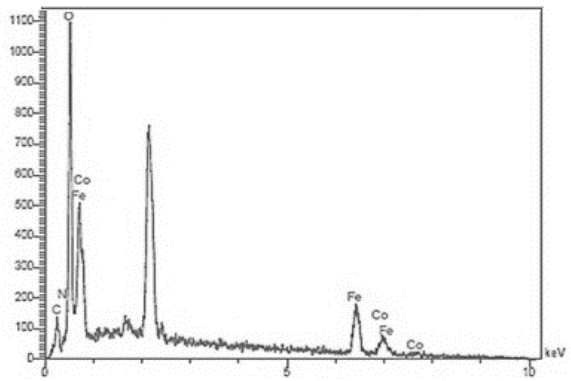

Figure 4. EDX spectrum of S_2.

The magnetic hysteresis loop of the as-prepared coated $CoFe_2O_4$ is investigated by VSM (Fig. 5). According to the hysteresis loop of cobalt ferrite nanomaterial, it has residual magnetism when it is inserted in the magnetic field bar. As a result, the sample shows ferromagnetic behavior at room temperature and has a saturation magnetization of 59 emu/g.

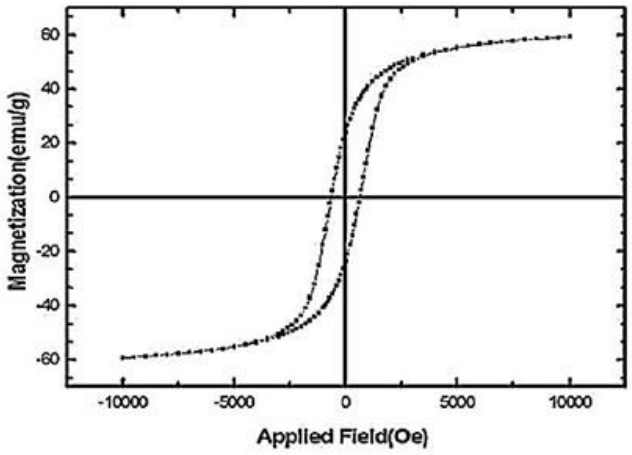

Figure 5. VSM curve of S_1.

3.2. Anti-cancer study

3.2.1. Growth and viability inhibition of K562 cells

The effect of different concentrations of (0-12 µM) cobalt ferrite nanoparticles were examined at time intervals of 24, 48 and 72 h. The range of concentrations was obtained after several tests. In a typical test, we studied the toxicity of coated cobalt ferrite nanoparticles (S_2) on the cells. For this purpose, 2×10^4 cells per well were cultured and treated with different doses of the nanoparticles. After the desired time, IC_{50}, a certain concentration of oleic acid coated cobalt ferrite nanomaterial inhibiting the growth and proliferation of cells by 50%, was determined by MTT assay. Fig. 6, shows the viability percent of the cells after treatment with different concentrations of cobalt ferrite nanoparticles. As seen in Fig. 6, inhibition of growth and viability of K562 cells depends on time and the nanoparticle dose. After 72 h, a concentration of 9 µM resulted in 50% inhibition of growth and viability of K562 cells (IC_{50} concentration).

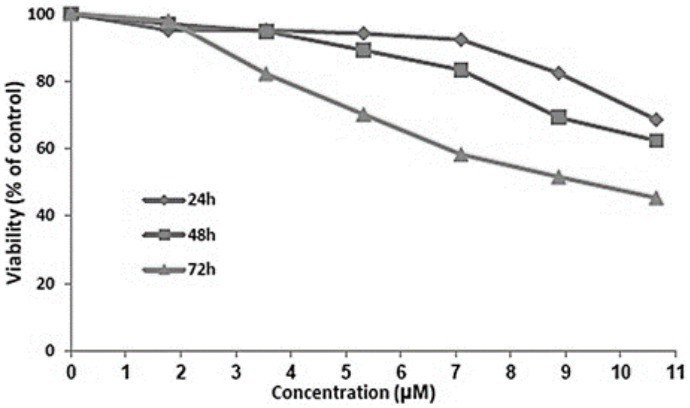

Figure 6. Viability of the K562 cells treated with different concentrations (0-12 µM) of cobalt ferrite nanoparticles (S_2).

3.2.2. Apoptosis study using an optical microscope

Optical images of the experiments show the significant changes in K562 cells treated with cobalt ferrite nanoparticles at different times. After 24 h treatment of K562 cells with IC_{50} (9 µM of cobalt ferrite nanoparticles), inhibition of cell growth is observed. When the cells are opposed with IC_{50} for 48 and 72 h, the apoptosis and dead cells are detectable, respectively. These observed changes occurred due to introducing the nanomaterials in the medium to confirm the effect of the nanomaterials on the cancer cells growth.

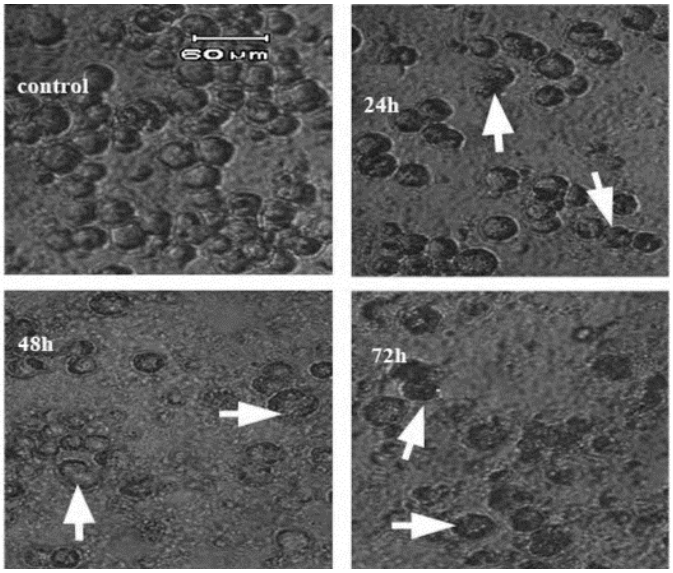

Figure 7. Images of optical microscopy for visual changes of K562 cells treated with cobalt ferrite nanoparticles used to evaluate the occurrence of apoptosis (white arrows) after 24 to 72 h.

3.2.3. Apoptosis study using fluorescence microscopy

Because ferrites are biological materials and show no toxicity in environment, so they can be used in biological medium. $CoFe_2O_4$ can be used to remove cancerous cells in a biological environment effectively because it is possible to produce high purity and of nano sized compounds by controlling the synthesis method. As a result, the anticancer effect of the new nanoparticles on the K562 cell line by in vitro model of blood cancer (type CML) is investigated [35,36].

To study the induction of apoptosis in K562 cells by cobalt ferrite nanoparticles, changes in apoptotic morphology were examined by comparing the control and treated cell groups by fluorescence microscopy at early and advanced stages at 72 h treatment time.

In the images of the groups treated by the nanomaterial, the control group cells shown by green color (Fig. 8a) are compacted and changed to bright spots in the nucleus of cells (early apoptosis) (Fig. 8b). The wrinkled and sliced cells (late apoptosis) are seen in yellow color. As shown in the Figure, after the treatment of K562 cells with 9 µM of cobalt ferrite nanoparticles (S_2) for 72 h, the final stages of apoptosis were achieved and the formation of apoptotic bodies was occurred. The shrinkage and yellow cells with condensed nuclei, assigned by white arrows, confirm the influence of the nanomaterials on the cancerous cells.

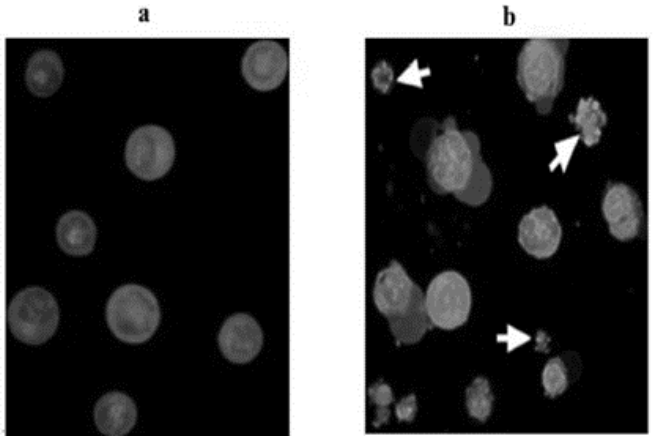

Figure 8. Fluorescent microscope image of K562 cells to evaluate the occurrence of apoptosis. In Untreated cells (control) showed by green color (**a**), and treated cells by cobalt ferrite nanoparticle (**b**). Shrinkage of the membrane and formation of apoptotic bodies shown by yellow color are displayed by white arrows.

4. CONCLUSIONS

In the present research, the cobalt ferrite nanoparticles were synthesized by a simple co-precipitation method. The research work focused on preparing coated $CoFe_2O_4$ nanoparticles and investigating their properties as magnetic drug carriers. These nanoparticles as the core were coated with a thin crust of 45% oleic acid through co-precipitation method to produce core-shell nanostructures. SEM images confirmed that the as-prepared cobalt ferrite nanomaterials were in nano scale. The VSM results showed that the coated $CoFe_2O_4$ had ferromagnetic behavior with the saturation magnetization of 59 emu/g at room temperature. Cobalt ferrite nanoparticles toxicity on K562 cells was examined.

To investigate the effects of cobalt ferrite nanoparticles, the colorimetric MTT test was used. It was found that the inhibition of growth and viability of K562 cells was depended on the nanoparticle dose and treatment time. The anticancer data showed that the coated nanoparticles induced cell death in K562 cells. In general, we found that cobalt ferrite nanoparticle had the ability of growth inhibition and apoptosis induction of leukemia cancer cell line K562. The as-synthesized coated compound showed strong apoptotic effects on K562 cell line as a model of CML at 72 h with 9 μM of the coated $CoFe_2O_4$. In general, the behavior of this compound for induction of apoptosis made it a good candidate for future pharmacological studies for treatment of leukemia.

ACKNOWLEDGEMENTS

The authors appreciate Urmia University and University of Tabriz for conducting the research tests.

REFERENCES

1. V. Kesavan, P.S. Sivanand, S. Chandrasekaran, Y. Koltypin, A. Gedanken, *Angew Chem. Int. Ed*. **38**, 3521 (1999).
2. L.H. Huo, W. Li, L.H. Lu, H.N. Cui, S. Q. Xi, J. Wang, B. Zhao, Y.C. Shen, Z.H. Lu, *Chem. Mater*. **12**, 790 (2000).
3. K. Suresh, K. C. Patil, *J. Mater. Sci. Lett.* **12**, 572 (1993).
4. M. Kroell, M. Pridoehl, G. Zimmermann, L. Pop, S. Odenbach, A. Hartwig, *J. Magn. Mater.* **289**, 21 (2005).
5. K.C. Patial, M.S. Hegde, T. Rattan, T. Aruna, *Chemistry of Nano Crystalline Oxide Materials, Combustion Synthesis, Properties and Applications*, Published by World Scientific Published Co. Pte. Ltd, 2008.
6. J.E. Kim, J.Y. Shin, M.H. Cho, *Arch. Toxicol.* **86**, 685 (2012).
7. V.P. Torcilin, Nanoparticulates as drug carriers, 1st Edition, Imperial College Press, 2006.
8. J. Ding, P.G. McCormick, R. Street, Solid State Commun. **95**, 31 (1995).
9. K. Maaz, A. Mumtaza, S.K. Hasanain, A. Ceylan, *J. Magn. Magn. Mater.* **308**, 289 (2007).
10. Pui, D. Gherca, G. Carja, *Dig. J. Nanomater Biostruct.* **6**, 1783 (2011).
11. F. Liu, S. Laurent, A. Roch, L.V. Elst, R.N. Muller, *J. Nanomater.* **2013**, 1 (2013).
12. S.R. Ahmed, P. Kofinas, *Macromolecules.* **35**, 3338 (2002).
13. Y. Liu, Y. Zhang, J.D. Feng, C.F. Li, J. Shi, R. Xiong, *J. Exp. Nanosc.* **4**, 159 (2009).
14. S. Sathiya, K. Parasuraman, M. Anbarasu, K. Balamurugan, *Nano Vision.* **5**, 133 (2015).
15. F. Mansouri, G. Amiri, M. Fatemi, *Nanomed J.* **3**, 196 (2016).
16. F. Huixia, C. Baiyi, Z. Deyi, Z. Jianqiang, T. Lin, *J. Magn. Magn. Mater*. **356**, 68 (2014).
17. Z. Zi, Y. Sun, X. Zhu, Z. Yang, J. Dai, W. Song, *J. Magn. Magn. Mater*. **321**, 1251 (2009).
18. M. Houshiar, F. Zebhi, Z.J. Razi, A. Alidoust, Z. Askari, *J. Magn. Magn. Mater*. **371**, 43 (2014).
19. G. Sheet, A.R. Cunliffe, E.J. Offerman, C.M. Folkman, *J. Appl. Phys.* **107**, 104309 (2010).
20. V.L. Othéro de Brito, S.A. Cunha, L.V. Lemos, C.B. Nunes, *Sensors.* **12**, 10086 (2012).
21. S. Pauline, A.P. Amaliya, *Arch. Appl. Sci. Res.* **3**, 213 (2011).
22. Z. Zhou, Y. Zhang, Z. Wang, W. Wei, W. Tang, J. Shi, R. Xiong, *Appl. Surf. Sci.* **254**, 6972 (2008).
23. G.R. Amiri, S. Fatahian, A.R. Jelvani, R.M. Dehaghi, M. Habibi, *Adv. Mater Rapid. Commun.* **5**, 1178 (2011).
24. K.S. Rao, G.S.V.R.K. Choudary, K.H. Rao, C. Sujatha, *Proced. Mater. Sci*. **10**, 19 (2015).
25. W.P. Wang, H. Yang, T. Xian, J.L. Jiang, *Mater Trans.* **53**, 1586 (2012).
26. C. Sun, J.S.H. Lee, M. Zhang, *Adv. Drug Deliv. Rev*. **60**, 1252 (2008).
27. Z. Dai, R.C. Quackenbush, K.D. Courtney, M. Grove, D. Cortez, G.W. Reuther, A.M. Pendergast, *Genes Dev.* **12**, 1415 (1998).
28. R.T. Maziarz, M.J. Mauro, *Bone Marrow Transplant.* **32**, 459 (2003).
29. D. Fabbro, S. Ruetz, E. Buchdunger, S.W. Cowan-Jacob, G. Fendrich, J. Liebetanz, J. Mestan, T. O'Reilly, P. Traxler, B. Chaudhuri, H. Fretz, J. Zimmermann, T. Meyer, G. Caravatti, P. Furet, P.W. Manley, *Pharm. Therap.* **93**, 79 (2002).
30. S.I. Han, Y.S. Kim, T.H. Kim, *BMB reports.* **41**, 1 (2008).
31. A. Russo, M. Terrasi, V. Agnese, D. Santini, V. Bazan, *Ann. Oncol.* **17**, vii115 (2006).
32. H. Guo, X. Yang, T. Xiao, W. Zhang, L. Lou, J. Mugnier, *Appl. Sur. Sci.* **230**, 215 (2004).
33. G. Baldi, D. Bonacchi, M.C. Franchini, D. Gentili, G. Lorenzi, A. Ricci, C. Ravagli, *Langmuir*. **23**, 4026 (2007).
34. B. Babić-Stojić, V. Jokanović, D. Milivojević, Z. Jagličić, D. Makovec, N. Jović, M. Marinović-Cincović, *J. Nanomater.* **2013**, 1 (2013).
35. S. Hyewon, H. Oh, C. Lee, *J. Microbiol Biotechnol.* **152**, 540 (2011).
36. S. Jeong, M. Han, C. Jin, G. Kim, B. Choi, T. Nam, S. Kim, Y. Choi, *Int. J. Mol. Med.* **25**, 31 (2010).